Biodegradable Barrier Membranes Based on Nanoclays and Carrageenan/Pectin Blends

Isabel M. Coelhoso[1,*], Ana Rita V. Ferreira[1] and Vítor D. Alves[2]

[1]*Requimte/CQFB, Departamento de Química, Faculdade de Ciências e Tecnologia, Universidade Nova de Lisboa, Campus de Caparica, 2829-516 Caparica, Portugal*

[2]*CEER – Centro de Engenharia dos Biossistemas, Instituto Superior de Agronomia, Universidade de Lisboa, Tapada da Ajuda, 1349-017 Lisboa, Portugal*

Abstract: The aim of this work is the study of the barrier properties of biodegradable membranes based on commercial pectin and kappa-carrageenan and organically modified nanoclays. Membranes (67% k-carrageenan, 33% pectin) with different amounts of nanoclays (1, 5 and 10%) were prepared by the solution intercalation method and casting. The films exhibited enhanced gas and water vapour barrier properties when compared to the ones without nanoclay particles. A water vapour permeability reduction of 35% for a nanoclay loading of 10 % was observed. The positive impact on the films' barrier properties of the organic nanoclay particles inclusion, results from a combined effect of increased tortuosity and reduction of water sorption due to the hydrophobic nature of the clay. The permeability to carbon dioxide has been significantly reduced (50% reduction for 1% nanoclay content).

Scanning electron microscopy coupled with energy dispersive X-ray spectroscopy analysis indicated the presence of under exfoliated nanoclay aggregates at 10%. The membranes have also shown a decrease of their stiffness and an increase of the elongation at break with the inclusion of nanoclay particles. An attenuation of the membranes transparency was observed, however, the colour measured after the application of test membranes on coloured paper sheets, did not change significantly with the inclusion of nanoclay particles.

Keywords: Biodegradable membranes, Pectin-carrageenan blends, Nanocomposites, Barrier properties

1. INTRODUCTION

There is an urgent need of better polymer-based barrier materials for limiting oxygen transference into food products, pharmaceuticals, and particularly sensitive electronic components like displays based on organic light-emitting diodes [1, 2].

Polysaccharide membranes are considered effective barriers against gases (oxygen and carbon dioxide) due to their hydrogen-bonded dense polymer matrix. However, their hydrophilic nature restricts their moisture barrier properties, significantly limiting their use. Moreover, their mechanical properties are not satisfying for all membrane applications. Hence, there have been many studies to improve the mechanical properties of polysaccharide-based membranes either using blends of different polymers or incorporating hydrophobic materials and plasticizers [3].

Enhancement of barrier properties due to increased tortuosity is a promising feature of biopolymer-clay nanocomposites and, in addition, they present a large improvement in the mechanical and physical properties compared with pure polymer or conventional composites [4-11].

The clays contain usually hydrated sodium or potassium ions, which can be replaced by the alkylammonium and alkylphosphonium ions. The organic modifier plays an important role for producing the nanocomposite because it may favour the intercalation of the polymer chain by dictating the gallery spacing [12]. The insertion of alkylammonium or alkylphosphonium cations into the galleries increases the inter layer spacing which promotes the intercalation of polymer chains into the galleries during nanocomposite preparation.

A variety of polysaccharides and their derivatives have been used as biodegradable film-forming matrixes. They include starch, cellulose, alginate, pectin, carrageenan, chitosan, and various gums [13]. In particular, pectin obtained from food processing industry wastes and carrageenan from seaweeds, have a particular interest, since they provide new markets for low valued sustainable resources.

In a previous work it was already stated that blends of kappa-carrageenan and pectin are able to form cohesive and transparent membranes [14]. It was shown that, their hydrophilic character increases with increasing kappa-carrageenan content in the polymer matrix, but reached a plateau at about 67% (dry basis) of kappa-carrageenan.

*Address correspondence to this author at the Requimte/CQFB, Departamento de Química, Faculdade de Ciências e Tecnologia, Universidade Nova de Lisboa, Campus de Caparica, 2829-516 Caparica, Portugal; Tel: +351 212948302; Fax: + 351 212948550; E-mail: imrc@fct.unl.pt

In order to enhance the water resistance and barrier properties of these films, inorganic impermeable particles (mica flakes) were included in the polymer matrix [15]. The permeability to water vapour and to gases was reduced with the addition of mica particles until a critical amount of 10% above which, there was a decrease of the barrier properties.

This high quantity of particles in the films makes them less transparent and not very attractive for packaging applications. This drawback can be overcome reducing the size and the amount of the particles to be included in the films.

The aim of this work is the study the barrier properties of pectin and kappa-carrageenan membranes using organically modified nanoclays (Nanomer® 1.34 TCN). The hygroscopic properties and water vapour and gas transport through the composite membranes, with different nanoclay content, were evaluated. The morphological and chemical composition of the membranes and the dispersion of the nanoclays were determined by scanning electron microscopy coupled with energy dispersive X-ray spectroscopy analysis (SEM/EDXS). The effect of incorporating nanoclay in the polymer matrix on the transparency and on the mechanical properties of the membranes was also investigated.

2. MATERIALS AND METHODS

2.1. Films Preparation

Commercial kappa-carrageenan and pectin from citrus fruit (Sigma Aldrich, Spain) and nanoclay particles (Nanomer® 1.34 TCN, montmorillonite clay surface modified with 25-35 wt % methyl dihidroxyethyl hydrogenate tallow ammonium - OMMT), were used to prepare carrageenan-pectin-clay films, by the solution intercalation method. The polymer is dissolved in a solvent (*i.e*. water) and the clay is dispersed in the same solvent. As the clay is swollen the polymer chains intercalate between the layers of the clay.

Nanoclay particles (1%, 5%, 10%, g nanoclay/ 100g dry polymer) were dispersed in deionised water (30ml) containing sodium azide (10 mg/L) to prevent microbial growth. The clay suspension was mixed for 1 h using a magnetic stirrer and sonicated for 30 min in a bath-type ultrasound sonicator (Bandelin sonorex super RK25577). After that, 0.6 g of dry polymer (66.7% commercial kappa-carrageenan and 33.3% pectin) were added to the nanoclay solution and heated to 90 ºC under stirring during 20 minutes. The solution was transferred to a Teflon dish after the removal of air bubbles from the viscous medium under vacuum. The cast solution was dried at 30 ºC to form a membrane and its thickness was measured at different points using a manual micrometer (Braive Instruments, Belgium).

2.2. Scanning Electron Microscopy

The morphological and chemical composition of the membranes, as well as the dispersion of the nanoclays, were obtained by scanning electron microscopy coupled with energy dispersive X-ray spectroscopy (SEM/EDXS), using a field emission scanning electron microscope (Jeol JSM-700IF). A gold coating with a thickness of a few nanometers was deposited on samples surface before their observation.

2.3. Colour Measurements and Transparency

The colour of pectin/carrageenan membranes and the colour alteration on coloured papers due to the application of those membranes was evaluated with a Minolta CR-300 colorimeter, USA, based on the CIE Lab colour model. The parameters L* (luminosity), a* (hue between red and green) and b* (hue between yellow and blue) were measured.

Five measurements on different areas of coloured paper sheets covered with the membranes with different nanoclay content, were performed, and the difference of colour was calculated according to the following equation:

$$\Delta E_{ab} = \left[(\Delta L^*)^2 + (\Delta a^*)^2 + (\Delta b^*)^2 \right]^{1/2} \quad (1)$$

Where $\Delta L^* = L^* - L_0^*$, $\Delta a^* = a^* - a_0^*$ and $\Delta b^* = b^* - b_0^*$, where L_0^*, a_0^* and b_0^* are the parameters of colour standards (coloured paper covered by membranes without nanoclays) and L*, a* and b* are the values measured for coloured paper covered by membranes with nanoclays. In addition, transparency of the membranes was calculated as follows:

$$\text{Transparency} = -\log\left(\frac{T_{600}}{x}\right) \quad (2)$$

Where T_{600} is the transmittance at 600 nm and *x* is the membrane thickness (mm). The transmittance of film samples at 600 nm was measured using the spectrophotometer Heλos α (Thermo Spectronic, UK).

2.4. Mechanical Tests

Tensile tests were carried out using a TA-XT plus Texture Analyser (Stable Micro Systems, U.K.). Membrane strips (70x20mm) were mounted in the tensile grips A/TG and stretched at a speed of 0.5 mm/s in tension mode. Tensile properties were calculated plotting the stress (tensile force / initial film cross-sectional area) versus strain (elongation as a fraction of the initial length). Before analysis, the samples were conditioned at 52.7% RH and 19ºC. At least five replicates of each membrane were analysed.

2.5. Water Sorption Isotherms

Water sorption isotherms were determined by the gravimetric method. Membrane samples with dimensions of 25x25 mm were dried at 70 ºC during 24 h. Then, the samples were weighed and then placed in desiccators with different relative humidity values, imposed by the use of saturated saline solutions. The experiments were carried out at 30 ± 2 ºC using solutions of LiCl, CH_3COOK, K_2CO3, $Mg(NO_3)_2$, $NaNO_2$, $(NH_4)_2SO_4$, $BaCl_2$ and K_2SO_4, which have water activities (a_w) of 0.115, 0.225, 0.447, 0.52, 0.649, 0.806 , 0.92 and 0.977, respectively. The samples were weighed again after being equilibrated for 3 weeks. The Guggenheim-Anderson-de Boer (GAB) model was used to fit the experimental sorption data:

$$X = \frac{CkX_0 a_w}{\left[\left(1-ka_w\right)\left(1-ka_w+Cka_w\right)\right]} \quad (3)$$

where X is the equilibrium moisture content at the water activity a_w, X_0 is the monolayer moisture content and represents the water content corresponding to saturation of all primary energy difference between the water molecules attached to primary sorption sites and those adsorption sites by one water molecule, C is the Guggenheim constant and represents the absorbed to successive sorption layers, and k is the corrective constant taking into account properties of multilayer molecules with respect to the bulk liquid. GAB equation parameters were calculated by non-linear fitting using the software package Scientist™, from MicroMath®.

2.6. Water Vapour Permeability

The methodology used was based in the ASTM E-96-80 (1996). Membranes were sealed with silicone to the top of a glass cell with a diameter of 5 cm. The driving force tested was imposed using a saturated $BaCl_2$ solution (RH = 92%) inside the cell and a saturated $NaNO_2$ solution outside (RH = 64.9%), in a desiccator. The membranes were previously equilibrated at a relative humidity of 92%. A fan was used to promote the circulation of air inside the desiccator, in order to minimize the mass transfer resistance of the air boundary layer above the test membrane. The room temperature and the relative humidity outside the cell were measured over time using a thermohygrometer (Vaisala, Finland). The water vapour flux was determined by weighing the cell in regular time intervals for 5-6 hours.

2.7. Gas Permeability

The experimental apparatus used is composed of a stainless steel cell with two identical chambers separated by the test membrane, as described in our previous experiment [15]. The membranes were equilibrated at a constant relative humidity in order to possess a water content of 20% (dry basis) in the beginning of each experiment. The permeability was evaluated by pressurizing one of the chambers (feed) up to 0.7 bar, with pure carbon dioxide (High-purity grade 99.998%, Praxair, Spain) followed by the measurement of the pressure change in both chambers over time, using two pressure transducers (Druck PDCR 910, England). The measurements were made at constant temperature, 30ºC, using a thermostatic bath (Julabo EH, Germany).

3. RESULTS AND DISCUSSION

3.1. Morphology and Chemical Composition of the Membranes

The morphology and chemical composition of the membranes as well as the dispersion of the nanoclay particles, were obtained by SEM/EDXS. It was observed that the OMMT is homogeneously dispersed in the matrix of the samples with lower OMMT content (1%). However, when the OMMT loading is higher, apparent aggregation is observed, indicating a heterogeneous dispersion of the clay particles. Figure **1** shows a SEM image of a membrane with the higher nanoclay content studied (10%), along with the spatial distribution of silicium and aluminium, which are elements present on OMMT chemical composition.

Poorly dispersed particles with a size on the micrometer range are observed on the SEM image (Figure **1A**). The regions where silicium and aluminium atoms are more concentrated (white spots on Figures **1B** and **1C**, respectively) coincide with the particles on

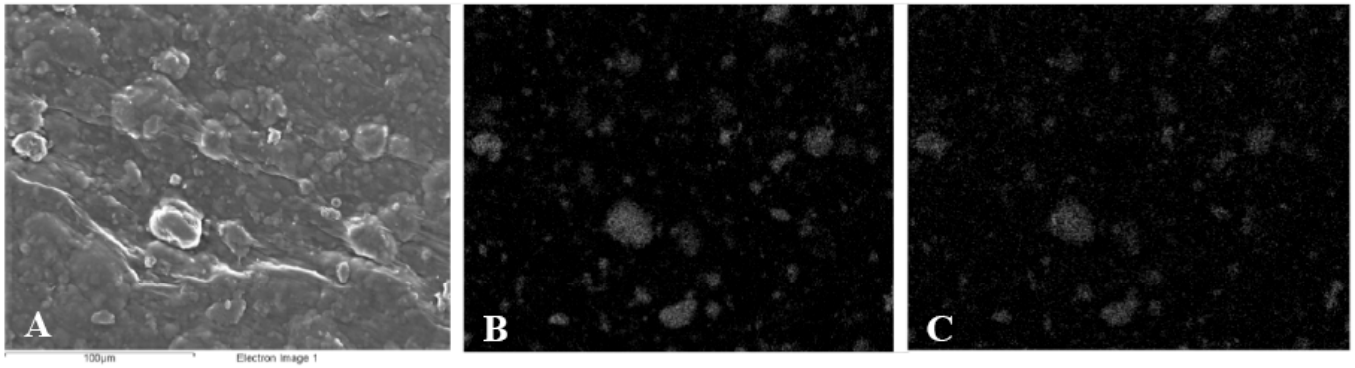

Figure 1: Morphology of a 10% nanoclay membrane sample: **(A)** SEM image, **(B)** EDXS for silicium, **(C)** EDXS for aluminium.

the SEM image. This fact indicates the presence of inefficiently exfoliated nanoclay aggregates.

Although exfoliated polymer-clay nanocomposite membranes are especially desirable, complete exfoliation is very difficult to achieve and most polymer-clay nanocomposites exhibit regions where partially intercalated and exfoliated structures coexist [16].

3.2. Membranes Appearance and Transparency

The membranes prepared present a thickness of 50±5 µm. The transparency values obtained for membranes with different nanoclay content, according to Eq. (2), are presented in Table **1**.

The value of T_{600} increased as more nanoclay particles were added to the polymer matrix, which indicates an attenuation of the films transparency. However, the colour measured after the application of test membranes on coloured paper sheets, did not change substantially with increasing the nanoclay particles content, as the maximum ΔE value observed was 3.9±0.4 (Table **1**). These results reveal that, the assessment of how membranes can affect colour perception should not be inferred only by using Eq. (2), which is limited to the evaluation of absorption of a single wavelength.

3.3. Mechanical Properties

The membranes are flexible and tough and could be easily bended without breaking. The mechanical properties of hydrophilic matrices are quite dependent on their water content, which is related to the ambient relative humidity (RH). As so, all samples were conditioned at the same RH (52.7%) and temperature (19ºC) before analysis. Figure **2** shows typical stress-strain curves obtained from tensile tests. It may be observed that the membranes became less stiff when stretched axially, as more nanoclay particles were added to the polymeric matrix.

This behaviour is confirmed by a decrease of the calculated Young modulus and an increase of strain at break (Table **2**).

3.4. Water Sorption Isotherms

The water sorption isotherms of the samples obtained for the carrageenan/pectin mixture (67% carrageenan), varying the content of the organically modified nanoclays (1, 5 and 10%), are presented in

Table 1: Transparency and Colour Alteration Values Induced by the Application of Membranes on Coloured Paper Sheets

Nanoclay content	*Transparency*	ΔE				
		White	Green	Red	Blue	Yellow
0%	3.0±0.7	-	-	-	-	-
1%	5.4±1.8	2.8±0.1	2.2±0.2	1.5±0.2	1.7±0.4	1.6±0.2
5%	10.9±1.2	3.2±0.3	2.5±0.4	2.1±0.3	3.5±1.1	2.4±0.2
10%	15.1±1.3	2.7±0.2	2.8±0.3	2.6±0.1	3.9±0.4	2.8±0.1

Figure **3**. Experimental data were fitted to GAB equation and the estimated parameters are shown in Table **3**.

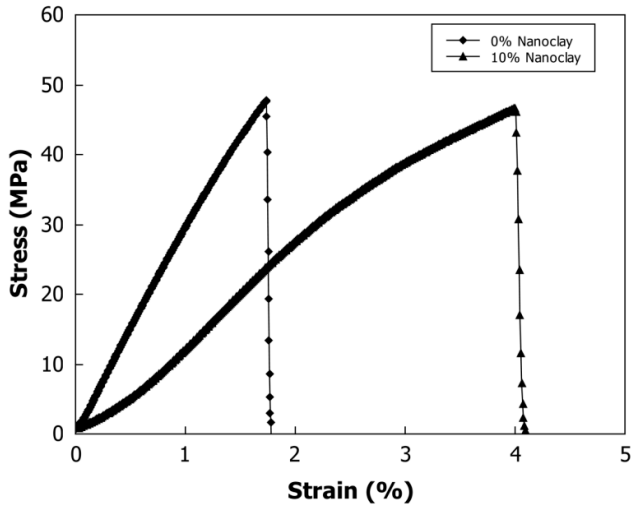

Figure 2: Effect of nanoclay content on membranes' tensile properties: typical stress-strain curves.

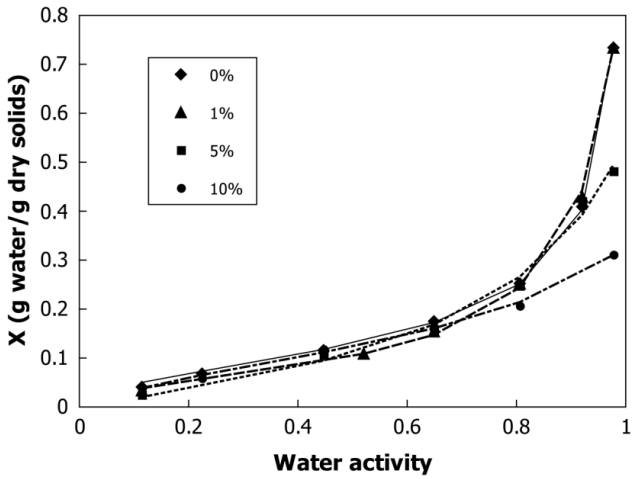

Figure 3: Moisture sorption isotherms of kappa-carrageenan/pectin membranes with different amounts of nanoclay. The lines represent the fitted GAB curves.

The equilibrium moisture is independent of the amount of nanoclay for a_w values up to 0.6, increasing slowly with a_w, followed by a steep rise. The water adsorption capacity of the membranes for a_w values higher than 0.8 decreases with the amount of particles added. This behaviour should be expected for hydrophobic particles, indicating that they are repelling water, especially for high water activities.

This is in contrast of what happened in a previous study with mica particles, where an increase of the sorption coefficient with the amount of mica particles was observed, due to their hydrophilic nature [15]. A similar behaviour was observed in a study comparing the water sorption using Cloisite Na^+ and Cloisite C30B, where the authors explain the significant reduction of the water sorption for Cloisite C30B, due its hydrophobicity [16].

3.5. Water Vapour Permeability and Diffusion Coefficients

The water vapour permeability (WVP) was calculated using Eq. (4):

$$WVP = \frac{N_w \times \delta}{\Delta P_{w,eff}} \quad (4)$$

In which, N_w is the water vapour molar flux, δ is the membrane thickness and $\Delta P_{w,eff}$ is the effective driving force, expressed as the water vapour pressure difference between both sides of the membrane, calculated taking into account the mass transfer resistance of the stagnant film of air below the membrane. The obtained value for $\Delta P_{w,eff}$ was 605±94 Pa, using the relative humidity difference of 92.0 – 64.9 % at 30 ± 1 ºC.

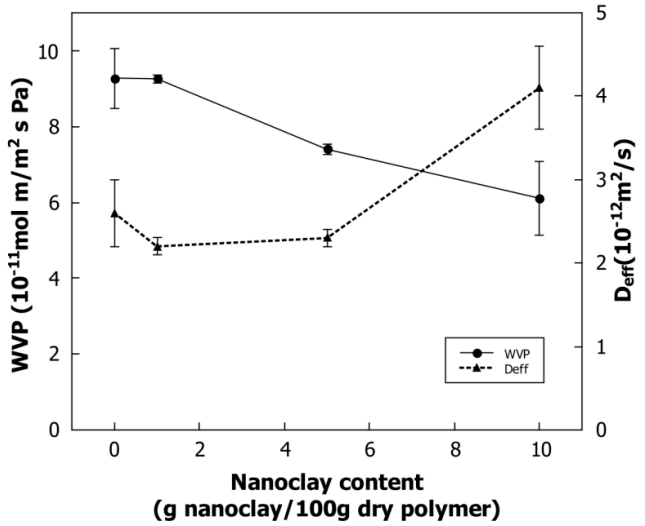

Figure 4: Water vapour permeability and effective water diffusion coefficient as a function of nanoclay content.

A pronounced decrease in WVP was observed (Figure **4**). It was reduced about 35% of its initial value, for 10% nanoclay content.

The permeability may be expressed as the product of the water sorption coefficient (*S*) and the effective water diffusion coefficient (D_{eff}). For the membranes studied, according to the water sorption isotherms

Table 2: Effect of Nanoclay Content on Membranes' Tensile Properties: Stress at Break, Elongation at Break and Young's Modulus

Nanoclay Content	Tensile Strength at Break (MPa)	Elongation at Break (%)	Young's Modulus (MPa)
0%	44.0 ± 5.2	1.7 ± 0.1	29.1 ± 0.9
1%	43.2 ± 3.4	2.7 ± 0.2	22.1 ± 0.5
5%	40.4 ± 5.2	2.0 ± 0.3	18.6 ± 3.0
10%	44.3 ± 3.3	4.2 ± 0.3	22.7 ± 3.0

Table 3: GAB Parameters of Fitted Curves of Moisture Sorption Isotherms

Sample	C	k	X_0	R^2
0% Nanoclay	8.21	0.88	0.089	0.991
1% Nanoclay	10.50	0.94	0.061	0.999
5% Nanoclay	1.39	0.80	0.154	0.983
10% Nanoclay	4.13	0.70	0.150	0.995

Table 4: Water Sorption Coefficients in Both Sides of the Films upon Water Vapour Permeability Measurements

S_i (10^{-4} g_{water}/g_{solids} Pa)	Nanoclay content			
	0%	1%	5%	10%
S_2	1.10	1.30	1.37	0.75
S_3	0.60	0.65	0.80	0.53

(Figure **3**), the sorption coefficient is similar for all the membranes tested, for water activities below 0.8. In this way, the major contribution for the differences encountered in the water vapour permeability values, for different nanoclay content, should be attributed to a variation of the effective diffusion coefficient. The same is not expected for water activity values above 0.8, for which membranes with higher nanoclay content (5% and 10%) presented a lower water adsorption at equilibrium.

The evaluation of D_{eff} and *S* was carried out using the methodology described in our previous work [15]. The effective diffusion coefficient is given by Eq. (5):

$$D_{eff} = \frac{N_W M_w}{\rho_s P_w^* \left(S_2 a_{w2} - S_3 a_{w3}\right)} \quad (5)$$

In which, N_w is the water vapour molar flux ρ_s is the dry membrane density, M_w is the water molar mass, S_i is the sorption coefficient [g_{water}/g_{solids} Pa], a_{wi} is the water activity of the liquid phase and P_w^* the pure water vapour pressure.

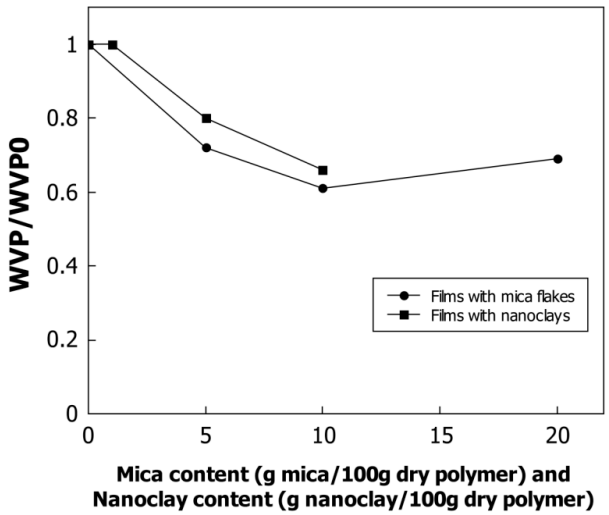

Figure 5: Water vapour permeability ratio as function of mica flakes [15]. and nanoclay loading.

The calculated effective diffusion coefficients are shown in Figure **4** and the estimated sorption coefficient values are presented on Table **4**. It can be observed that for nanoclay content below 5%, the

sorption coefficients in both membrane interfaces are similar for all membranes tested, while a decrease of the D_{eff} is detected. As such, the decrease of the WVP may be mainly attributed to a decrease of the water diffusion coefficient, due to the increase of tortuosity caused by the nanoclay particles. However, for the highest nanoclay content studied, a sharp increase of the D_{eff} is observed.

An increase in water diffusivity was also obtained for highly filled nanocomposite films of Cloisite C30B and polyamide due to the presence of aggregates, which favour the diffusion of water molecules along a new pathway consisting in a percolation path through the clay-polymer interfacial zones [16].

However, in this work, the WVP continued decreasing independently of the nanoclay content, which may be explained by the lower water sorption coefficient of the membranes with 10% particles, which compensated the higher D_{eff}, rendering a reduction on water vapour permeability. This is in contrast with the results obtained using hydrophilic particles (mica), where the WVP goes through a minimum, because there is an increase in both the diffusivity and the sorption coefficients with the increase of the amount of particles in the film, after a critical particle loading [15, 16].

The permeability reduction obtained for the films with organic nanoclays and mica particles is represented in Figure **5**. As it can be observed, the reduction is similar for the same amount of particles (nanoclay or mica) used. A WVP reduction of about 35% and 40 % was achieved for 10% nanoclay and mica flakes, respectively.

3.6. Gas Permeability

Regarding the barrier properties to carbon dioxide, the permeability was calculated using the following equation:

$$\frac{1}{\beta}\ln\left(\frac{\left[p_f - p_p\right]_0}{\left[p_f - p_p\right]}\right) = \frac{1}{\beta}\ln\left(\frac{\Delta p_0}{\Delta p}\right) = P\frac{t}{\delta} \qquad (10)$$

where p_f and p_p are the pressures in the feed and permeate compartments, respectively; P is the gas permeability; t is the time; and δ is the film thickness. The geometric parameter β is A ($1/V_f + 1/V_p$), where V_f and V_p are the volumes of the feed and permeate compartments, respectively, and A is the membrane area.

The measured permeability to carbon dioxide is presented in Figure **6**, along with the results obtained in a previous work [15], in which mica flakes were used instead of nanoclay particles. The results show that, in both cases, the permeability decreased significantly with the incorporation of the particles. In addition, a minimum value was observed for a specific particles content, after which it increased. The incorporation of nanoclay particles resulted on a more efficient barrier to carbon dioxide, as the minimum permeability value was achieved for a much lower particle loading (1%), compared to the one observed with mica flakes (10%). Even though the exfoliation of the nanoclay aggregates was incomplete, as perceived by SEM/EDX analysis, it was sufficient to generate particles with a higher specific area, resulting on more efficient barriers to gas diffusion. The observed increase on CO_2 permeability after a specific nanoclay loading is in agreement with other works referred in the literature concerning nanocomposite structures [17].

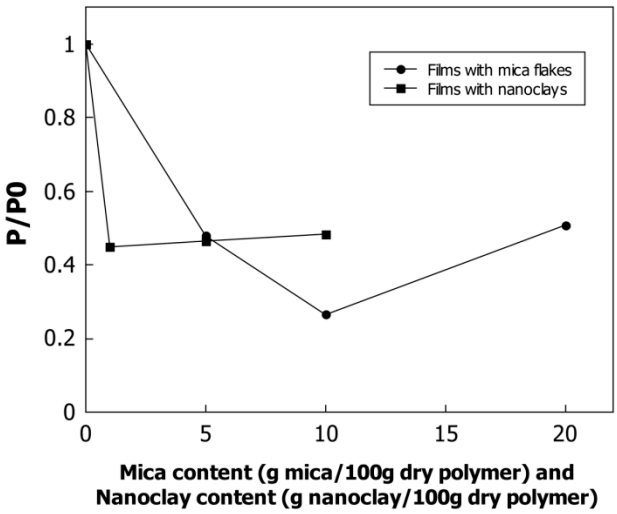

Figure 6: Carbon dioxide permeability ratio as function of mica flakes [15] and nanoclay loading.

This fact may be attributed to the creation of higher diffusion regions around the inorganic particles. These higher diffusion regions may be a consequence of the higher hydration of the polymeric matrix induced by the hydrophilic character of the mineral clays, when mica flakes were used. When organically modified nanoclays are present, higher diffusion zones may be formed due to the incompatibility between the nanoclays hydrophobic regions and the hydrophilic polymeric matrix. Above a certain clay content, the zones in which diffusion is higher will compensate the increase of diffusion path created by the impermeable barriers, leading to the rise of CO_2 permeability.

These results obtained are promising, since it was possible to increase the barrier properties to CO_2 of hydrated films (with 20% of water, dry basis), in conditions for which the polysaccharide films start to lose the good gas barrier properties that they possess when dried.

If we compare the permeability to carbon dioxide to that referred for synthetic polymers, we conclude that the inclusion of a nanoclay content of 1% on the kappa-carrageenan/pectin matrix plasticized with 20% (dry basis) of water ($P(CO_2)$ = 1.0x10^{-15} mol.m/m^2 s Pa), enabled to reach higher barrier properties than LDPE ($P(CO_2)$ = 4.2x10^{-15} mol.m/m^2 s Pa, [18]) and a similar value to that observed for PP ($P(CO_2)$ = 0.9x10^{-15} mol.m/m^2 s Pa, [19]).

4. CONCLUSIONS

In this work, the enhancement of the barrier properties to water vapour and CO_2 of a polymeric matrix composed by kappa-carrageenan and pectin (66.7% kappa-carrageenan), with the inclusion of organically modified nanoclays, was studied.

A WVP reduction of about 35% for a nanoclay content of 10 %, was observed. Up to a nanoclay content of 1%, this reduction was mainly due to a decrease of the effective water diffusion coefficient. On the other hand, for higher particles content (10%), the lower water sorption coefficient was the key factor for the water vapour permeability reduction.

A significant decrease of CO_2 permeability (50% for 1% nanoclay content) was also achieved. These results were obtained when the membranes were plasticized with water, for which there is a depletion of the good barrier properties characteristic of dry polysaccharide films.

Regarding the mechanical properties, the membranes have shown a decrease of their stiffness with the inclusion of nanoclay particles, illustrated by a decrease of the Young modulus and an increase of the strain at break.

It is envisaged that the positive impact of organically modified nanoclay particles on the membranes barrier and mechanical properties, may be further improved, by enhancing the particles dispersion and exfoliation degree.

ACKNOWLEDGEMENTS

The authors acknowledge Rocío Castelló for part of the experimental work performed during her training at FCT/UNL in the framework of the Erasmus program.

The authors would like to thank also Prof. Isabel Fonseca FCT/UNL for the help in the SEM/EDXS analysis.

REFERENCES

[1] Ferrari MC, Carranza S, Bonnecaze RT, Tung KK, Freeman BD, Paul DR. J Memb Sci 2009; 329: 183-192.

[2] Min H, Lee HS. Carb Lett 2014; 15: 50-56.

[3] Freitas F, Alves VD, Reis MA, Crespo JG, Coelhoso IM. J Appl Polym Sci 2014; 131*:* 40047.

[4] Bae HJ, Park HI, Hong SI, Byun YJ, Darby DO, Kimmel RM, *et al*. LWT-Food Sci Tech 2009; 42: 1179-1186.

[5] Choudalakis G, Gotsis AD. Eur Polym J 2009; 45: 967-984

[6] Cyras VP, Manfredi LB, Ton-That MT, Vázquez A. Carb Polym 2008; 73: 55-63.

[7] Fabra MJ, Talens P, Gavara R, Chiralt A. J Food Eng 2012; 109: 372-379.

[8] Magalhães NF, Andrade CT. Carb Polym 2009; 75: 712-718.

[9] Paul DR, Robeson LM. Polymer 2008; 49: 3187-3204.

[10] Pavlidou S, Papaspyrides CD. Progr Polym Sci 2008; 33: 1119-1198.

[11] Souza AC, Benze R, Ferrão ES, Ditchfield C, Coelho ACV, Tadini CC. LWT-Food Sci Tech 2012; 46: 110-117.

[12] Kumar S, Jog JP, Natarajan U. J Appl Polym Sci 2003; 89: 1186-1194.

[13] Siracusa V, Rocculi P, Romani S, Rosa M D Trends Food Sci Tech 2008; 19: 634-643.

[14] Alves V, Costa N, Hilliou L, Larotonda F, Gonçalves M, Sereno A, *et al* Desalination 2006; 199: 331-333.

[15] Alves V, Costa N, Coelhoso IM. Carb Polym 2010; 79: 269 - 276.

[16] Alexandre B, Langevin D, Méderic P, Aubry T, Couderc H, Nguyen QT, *et al*. J Memb Sci 2009; 328: 186-204.

[17] Cong H, Radosz M, Towler B F, Shen Y Sep Purif Tech 2007; 55: 281-291.

[18] Gontard N, Thibault R, Cuq B, Guilbert S. J Agric Food Chem 1996; 44: 1064-1069.

[19] Costamagna V, Strumia M, López-González M, Riande E. J Polym Sci Part B: Polym Phys 2007; 45 (17): 2421-2431

Received on 03-08-2014 Accepted on 30-08-2014 Published on 05-12-2014